RE-ENTRY PREDICTIONS FOR UNCONTROLLED SATELLITES: RESULTS AND CHALLENGES

Carmen Pardini[(1)], Luciano Anselmo[(2)]

[(1)] *Space Flight Dynamics Laboratory, ISTI/CNR, Via G. Moruzzi 1, 56126 Pisa, Italy (Carmen.Pardini@isti.cnr.it)*
[(2)] *Space Flight Dynamics Laboratory, ISTI/CNR, Via G. Moruzzi 1, 56126 Pisa, Italy (Luciano.Anselmo@isti.cnr.it)*

ABSTRACT

Currently, approximately 70% of the re-entries of intact orbital objects are uncontrolled, corresponding to about 50% of the returning mass, i.e. ~100 metric tons per year. On average, there is one spacecraft or rocket body uncontrolled re-entry every week, with an average mass around 2000 kg. Even though a detailed demise analysis is available only occasionally, in many cases the alert casualty expectancy threshold of 1:10,000 is probably violated.

Re-entry predictions are affected by various sources of inevitable uncertainty and, in spite of decades of efforts, mean relative errors of 20% often occur. This means that even predictions issued 3 hours before re-entry may be affected by an along-track uncertainty of 40,000 km (corresponding to one orbital path), possibly halved during the last hour. However, specific methods and procedures have been developed to provide understandable and unambiguous information useful for civil protection planning and applications.

1. RE-ENTRY STATISTICS

As of 3 April 2013, and since the decay of the Sputnik 1 launch vehicle core stage on 1 December 1957, 22,142 cataloged orbiting objects have re-entered the Earth's atmosphere [1]. About 67.9% were just operational debris, space junk and especially fragments of spacecraft and upper stage breakups or degradation, with an average Radar Cross Section (RCS) of 0.26 m^2. However, a substantial number was represented by intact objects, where most of the mass (> 99%, i.e. ~29,000 metric tons [2]) was concentrated: in fact, 16.3% (3619) were rocket bodies, with an average RCS of 14.17 m^2, 13.3% (2950) were spacecraft, with an average RCS of 25.76 m^2, and 2.5% (543) were platforms, used to support a payload while it is being placed into orbit, with an average RCS of 9.33 m^2. The re-entered spacecraft not associated with human spaceflight were 11.1% (2462) of the total, with an average RCS of 16.79 m^2. Altogether, the intact objects represented 32.1% of the re-entries, reduced to 29.9% by excluding the spacecraft either manned or supporting the human spaceflight programs (Tab. 1).

Approximately 76% of the upper stages re-entered so far belonged to Russia and Ukraine (see Fig. 1) and 17% to the United States (see Fig. 2). Far third was China, with less than 3%, followed by the European Space Agency (ESA) and Japan, with less than 2% each. Basically the same pattern applied to the re-entered spacecraft: about 65% belonged to the former Soviet Union, Russia and Ukraine, more than 29% to the United States, less than 2% to China and approximately 1% to Japan.

Table 1. Satellite re-entries: 1 Dec 1957 – 3 Apr 2013

Objects	Number	Average RCS (m^2)	RCS Sample
Spacecraft	2950 (13.3%)	25.76	46.7%
Spacecraft (unmanned programs)	2462 (11.1%)	16.79	44.5%
Rocket bodies	3619 (16.3%)	14.17	53.9%
Platforms	543 (2.5%)	9.33	42.5%
Intact objects	7112 (32.1%)	18.35	50.1%
Intact objects (no manned spacecraft)	6624 (29.9%)	14.71	49.5%
Debris	15,030 (67.9%)	0.26	65.9%
Cataloged objects	22,142 (100%)	5.31	61.2%

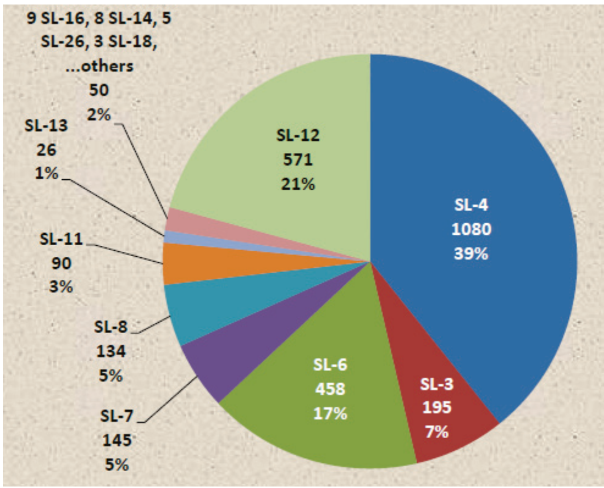

Figure 1. Re-entered orbital stages associated with Russian and Ukrainian launchers

Fig. 3 shows the yearly decay rate of debris, rocket bodies, spacecraft and platforms. The debris re-entry rate was subjected to wild variations, mostly as a result of specific fragmentation events. A further (minor)

Proc. Sixth IAASS Conference – Safety is Not an Option', Montreal, Canada 21–23 May 2013 (ESA SP-715, September 2013)

modulation was introduced by the thermospheric density variations induced by the 11-year solar activity cycle. The decay rate of intact objects, on the other hand, was mainly driven by the launch activity, again with a lesser, but not small, contribution from the solar cycle and the corresponding change in the magnitude of the drag perturbation (Fig. 4).

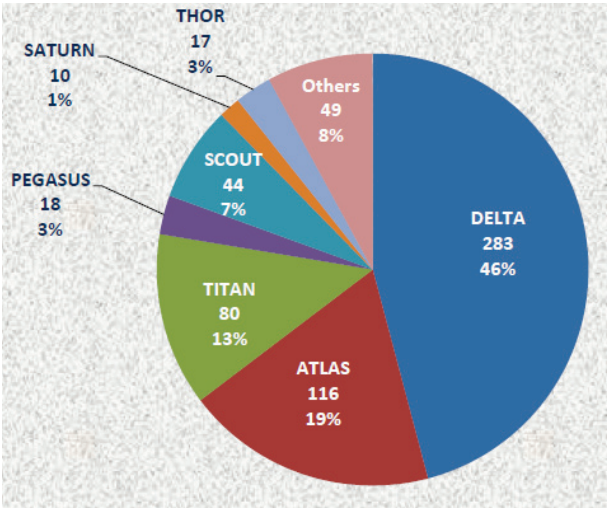

Figure 2. Re-entered orbital stages associated with American launcher families

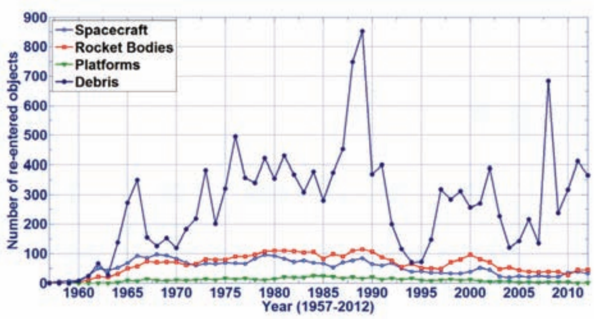

Figure 3. Yearly decay rate of cataloged objects

Figure 4. Yearly decay rate of intact objects compared to solar activity (in standard flux units at 10.7 cm)

If all the spacecraft associated with human spaceflight, i.e. manned spaceships and capsules, space stations, man-tended modules and cargo vehicles, are excluded from the tally, the resulting decay rate of intact objects is detailed in Fig. 5. At this scale the strong correlation with launch activity (Fig. 6) is even more evident, with the top rates which characterized the period between the mid-1960s and the end of the 1980s, the declining trend following the breakup of the Soviet Union, at the beginning of the 1990s, and the increasing number of commercial and emerging countries launches during the last 10-15 years.

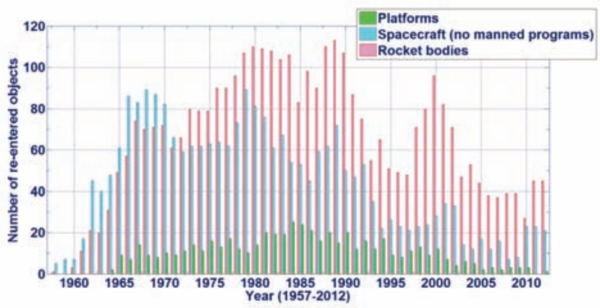

Figure 5. Yearly decay rate of intact objects excluding the spacecraft associated with the manned programs

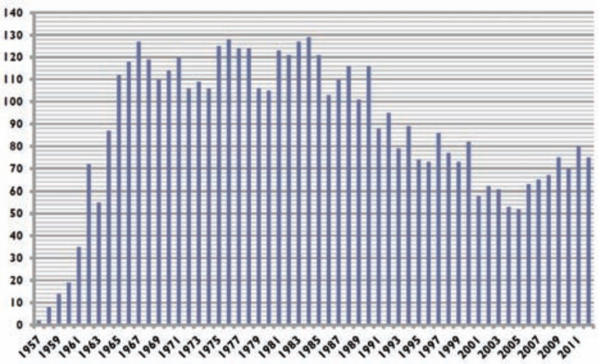

Figure 6. Yearly rate of actual orbital launches

Tabs. 2 and 3 detail the satellite re-entry yearly rates averaged over the last 55, 50, 40, 30, 20, 10 and 5 years. The numbers found show a systematic decreasing trend in the decay rate of intact objects over the last four decades, reflecting changes not only in the number of orbital launches but also in the mission profiles, with a growing fraction of spacecraft and rocket bodies placed in high Earth orbits. Moreover, during the last 15 years, a particularly long and deep solar activity minimum, bounded by two quite low maxima, surely played a role, with a corresponding reduction of atmospheric drag in low Earth orbits compared to previous decades.

Concerning the re-entry of cataloged debris, the averages are mostly affected by the fragmentation events, in particular catastrophic explosions and collisions, occurred in low Earth orbit at specific epochs. For this reason, they do not present a clear systematic trend, with averaged values between 250 and

400 decays per year.

A particularly interesting category of re-entered satellites is represented by the intact objects obtained by subtracting all the spacecraft associated with human spaceflight, which typically perform controlled re-entries. The corresponding averaged yearly, weekly and daily decay rates are detailed in Tab. 4. Regarding the re-entry of the spacecraft associated with human spaceflight, they represented so far the 16.5% of the re-entered spacecraft, the 7.4% of the re-entered spacecraft and rocket bodies and the 6.9% of the re-entered intact objects.

Table 2. Satellite yearly decay rate averaged over the last 55, 50, 40 and 30 years

Objects	55 yrs 1957-2012	50 yrs 1963-2012	40 yrs 1973-2012	30 yrs 1983-2012
Spacecraft	52.59	56.98	52.68	44.80
Spacecraft (unmanned programs)	43.91	47.56	41.93	32.80
Rocket bodies	64.48	71.48	75.08	68.50
Platforms	9.70	10.86	11.60	10.60
Intact objects	126.77	139.32	139.36	123.90
Intact objects (no manned spacecraft)	118.09	129.90	128.61	111.90
Debris	267.07	297.16	328.00	314.90

Table 3. Satellite yearly decay rate averaged over the last 20, 10 and 5 years

Objects	20 yrs 1993-2012	10 yrs 2003-2012	5 yrs 2008-2012
Spacecraft	32.80	25.90	29.60
Spacecraft (unmanned programs)	21.10	15.30	16.40
Rocket bodies	54.10	41.40	39.00
Platforms	6.50	2.80	2.00
Intact objects	93.40	70.10	70.60
Intact objects (no manned spacecraft)	81.70	59.50	57.40
Debris	254.30	285.50	402.60

Table 4. Average decay rate of intact objects, excluding the spacecraft associated with human spaceflight programs

Averaging Interval	Yearly rate	Weekly rate	Daily rate
1957-2012 (55 years)	118.09	2.26	0.323
1963-2012 (50 years)	129.90	2.49	0.356
1973-2012 (40 years)	128.61	2.46	0.352
1983-2012 (30 years)	111.90	2.14	0.306
1993-2012 (20 years)	81.70	1.57	0.224
2003-2012 (10 years)	59.50	1.14	0.163
2008-2012 (5 years)	57.40	1.10	0.157

2. UNCONTROLLED RE-ENTRIES

Even though it is clear that the potential risk posed on the ground and in mid-air by surviving components is a function of the re-entering object mass, so the debris can be generally neglected, the estimation of the number (and mass) of intact objects which re-entered in the atmosphere without control is not straightforward, because in addition to the spacecraft associated with the manned space programs and to other controlled re-entries carried out for safety reasons, several classified military reconnaissance programs systematically adopted controlled re-entries in order to recover capsules with exposed film or recorded data, or to prevent the accidental retrieval of secret spacecraft parts, revealing sensitive technologies, by potential hostile parties. Moreover, during the last few years there was a positive trend involving the controlled re-entry of upper stages as well: 3 in 2010, 8 in 2011 and 11 in 2012.

Anyway, a thorough and relatively intricate research was carried out in order to identify, to a reasonable level of confidence, all the spacecraft which performed controlled re-entries. In addition to de-orbited manned spaceships and capsules, man-tended modules, space stations, cargo vehicles and civilian spacecraft, the classified spacecraft and modules which accomplished controlled re-entries were identified as well, based on the information available in the open literature [3]. The results obtained are summarized in Fig. 7.

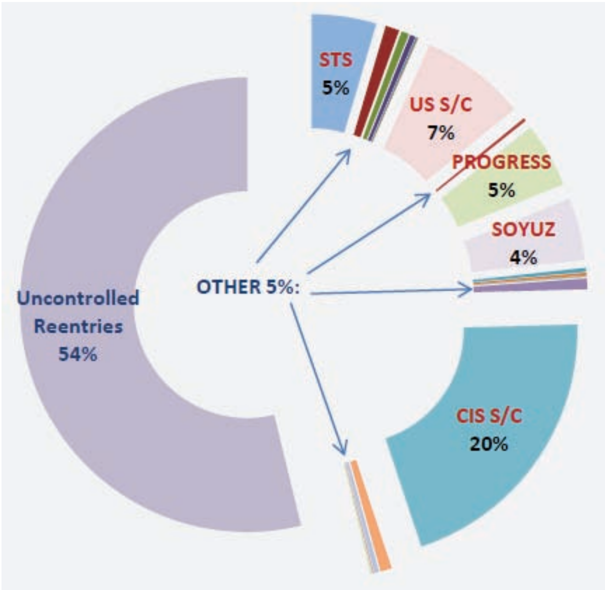

Figure 7. Estimate of spacecraft controlled re-entries

The surprising result was that about 46% of spacecraft re-entries were controlled in some way, leaving only a 54% completely uncontrolled. Adding the small number of controlled re-entries carried out by orbital upper stages, this means that the fraction of controlled re-entries among all the decayed cataloged objects was about 6.3%, 19.5% among the intact objects and 21.1% among spacecraft and rocket bodies. In other words, on average during the Space Age, one out of five re-entries of intact objects was controlled.

The total mass of the uncontrolled re-entered objects was assessed to be ~11,000 metric tons, mainly concentrated (> 98%) in almost 5700 intact objects, including nearly 5200 spacecraft (30.7%) and rocket bodies (69.3%). Excluding the Space Shuttle orbiters, during the last 15 years (1998-2012) the average re-entry mass flow of controlled and uncontrolled intact objects was around 180 metric tons per year, with a mean mass per object of approximately 2100 kg. Focusing the attention on the last 3 years (2010-2012), nearly 50% of the re-entering mass (around 590 metric tons in total, excluding again the Space Shuttle orbiters) was controlled. This accounted for about 30% of intact object re-entries (Space Shuttles included), mainly consisting of rocket bodies (52%) and spacecraft (46%). The average mass of the uncontrolled re-entering intact objects was around 1850 kg.

3. RE-ENTRY RISK EVALUATION

A satellite in circular orbit approaching re-entry has a specific mechanical energy of 3.2×10^7 J/kg. If all this energy were converted into heat entirely absorbed by the object, most materials would be totally vaporized. However, only a small fraction of this energy, typically around 1%, is usually absorbed by the re-entering body, so the chance of having surviving components hitting the ground is far from negligible, in particular when sizable spacecraft and rocket bodies are involved.

Detailed computer simulations and the analysis of retrieved spacecraft and rocket body components led to the conclusion that, also in the case of objects not specifically designed to survive the re-entry mechanical and thermal loads, a mass fraction between 5% and 40% of sufficiently massive bodies is able to reach the Earth surface [4][5]. Applying an average surviving fraction of 15-20% to the total amount of uncontrolled re-entered mass estimated in the previous section (~11,000 metric tons), it was found that around 1650-2200 metric tons of manmade orbital debris should have survived re-entry and hit the ground without control so far, with no confirmed case of personal injury.

In terms of mass, number and component survivability, the uncontrolled re-entries of spent upper stages generally present a higher risk on the ground compared to spacecraft and, except for very specific accidental cases, as the tragic loss of the Columbia Space Shuttle orbiter (2003), or the demise of Skylab (1979), the bulk of the re-entry fragments recovered so far on the ground comes from rocket bodies. This was probably one of the reasons, together with orbital debris mitigation, leading to the increasing practice of upper stage controlled de-orbiting during the last few years.

However, due to an expanding use of space and to a consequent rise in the amount of space hardware, the number of uncontrolled re-entries will remain significant in the foreseeable future. Taking also into account the concurrent increase of the world population, the ground casualty risk, even if remaining very small compared to other commonly accepted risks linked to the lifestyle or the workplace and household safety [6], will presumably show a tendency to grow in the coming years. For this reason, specific guidelines to minimize the risk to human life and property on the ground were defined. Re-entries compliant with the NASA standard 8719.14 [7] must have a human casualty expectancy [4] (i.e. the chance that anybody anywhere in the world will be injured by a piece of falling debris) lower than 1:10,000. Such alert threshold is now adopted by several organizations and countries around the world, even though only for a relatively small number of spacecraft and upper stages detailed breakup studies have been carried out, or disclosed to the public, in order to estimate their casualty expectancy [4][8]. Therefore, every week or two, on the average, an uncontrolled re-entry violating the above mentioned alert threshold probably occurs, unknown to most of the governments and safety authorities around the world.

Generally the overall casualty expectancy E_c is estimated using the following relationship:

$$E_c \cong \frac{NA_c}{4\pi R^2 \sin L_{\max}} \qquad (1)$$

where L_{max} is the maximum latitude, north or south, overflown by the re-entering satellite, R is the radius of the Earth, $4\pi R^2 \sin L_{max}$ is the area of the latitude band overflown by the satellite, N is the total population resident there and A_c is the total effective casualty area for the impacting fragments. The formula adopted by NASA to compute the effective casualty area due to a satellite re-entry is [4][7]:

$$A_c = \sum_{i=1}^{n}\left(\sqrt{A_h} + \sqrt{A_i}\right)^2 \qquad (2)$$

where $A_h = 0.36$ m^2 is the projected cross sectional area of a standing human and A_i is the cross section of each individual fragment reaching the ground.

The casualty expectancy for people in the open obtained with Eqs. 1 and 2 might be slightly refined taking into account winds, trajectory path angle, sliding, skidding or bouncing at ground impact, and splattering or cratering. In addition, debris carrying explosive, toxic or radioactive substances can significantly increase the casualty area. However, the surviving pieces of a re-entering satellite generally rain down vertically, with respect to the local horizon, during the last 10 km, with a relatively minor horizontal velocity component due to local winds. Moreover, any material able to explode or burn typically ignites or disperses at high altitude (several tens of kilometres), during the breakup phase. The latter fate usually occurs also to toxic liquids and radionuclides not stored in appropriately designed containment vessels. Concerning sliding, bouncing or splattering at ground impact, the three effects are generally exclusive and, because soft soil tends to be more common than hard surfaces, the effective casualty area computed using Eq. 2 might be, at most, enhanced by a factor 2 [9].

The human casualty risk associated with an uncontrolled re-entry can be subdivided in primary and secondary. The primary risk derives from the possibility of a direct hit of people in the open by a falling fragment. The secondary risk is instead associated with a potential debris impact on a building, a shelter, a high risk industrial plant (e.g. chemical or nuclear) or a vehicle (e.g. aircraft, ship, or train), possibly leading to indirect human casualties. The primary risk can be evaluated with Eqs. 1 and 2, taking into account that the debris kinetic energy threshold for any injury to the human body is 15 J, while a probability of fatality of 50% corresponds to a kinetic energy of 103 J [10]. Unfortunately there is no easy way to compute the secondary risk, also because a very small impact probability may be associated with potentially catastrophic consequences.

For people in buildings or shelters, the effective casualty area of a satellite surviving fragment may be larger or smaller than that computed with Eq. 2. The outcome depends on the fragment capability of penetrating or gravely damaging the sheltering structure. If this is not the case, the effective casualty area of the fragment becomes zero. In other words, concerning the sheltering of people or the protection of high risk industrial plants, attention should be paid to the fragment's capacity to penetrate and seriously damage the structure, to the excess kinetic energy retained by the impactor if penetration occurs, and to the falling structural debris produced by the impact. The same applies, basically, to oceanic ships and low velocity trains, while high velocity trains could also incur in the secondary consequences of a high velocity impact and/or derailment.

For airplanes in flight, moving around even at nearly 1000 km/h in the case of passenger jets, the problem is quite different, because even the impact with a debris practically at rest in the air could have severe consequences on board; in this case, the re-entering fragments mass and composition are more important, to assess the risk, than their kinetic energy in the ground reference frame. In order to estimate the total casualty expectancy for the commercial aircraft of registered carriers worldwide, let consider a surviving upper stage spherical tank, with a diameter of 1 m, re-entering the atmosphere from a sun-synchronous orbit. By applying Eq. 2 to people in the open and multiplying by the number of Earth inhabitants ($N \approx 7 \times 10^9$), the numerator of Eq. 1 becomes $NA_c \approx 1.54 \times 10^{10}$ m^2. If in Eq. 2 the projected cross sectional area of a standing human A_h is substituted with the estimated dorsal cross section of a typical airliner A_a, for instance an Airbus A320 ($A_a \approx 670$ m^2), and the average number of registered aircraft in the air over the world at any given time is assumed to be $N_a \approx 15{,}000$ [11][12], the numerator of Eq. 1 becomes $N_aA_a \approx 1.08 \times 10^7$ m^2. Therefore, $NA_c/N_aA_a \approx 1426$, and because $E_c << 1$, the probability of a flying aircraft hit by the re-entering rocket body tank is three orders of magnitude less than the probability to strike somebody anywhere in the world. Even considering an average of about 150 passengers per airplane and an absolutely catastrophic outcome for the potential impact, the effective passenger casualty expectancy would remain one order of magnitude less than the standard casualty expectancy computed for people in the open.

This conclusion still probably applies to all the other secondary risk situations as well. Therefore, Eqs. 1 and 2 applied in the standard way to people in the open, also taking into account all the uncertainties underlying the computation of the effective casualty area, provide the correct order of magnitude of the casualty expectancy for uncontrolled re-entry events, including much more complicated situations, as sheltered people or flying aircraft.

4. PREDICTION UNCERTAINTIES

After 55 years of space activity, predicting the re-entry time and location of an uncontrolled satellite remains a very tricky task. It can re-enter anywhere on a large portion of the Earth surface, putting all the locations within the latitude band defined by the orbit inclination into the risk zone. There is considerable uncertainty in the estimation of the re-entry epoch due to sometimes sparse and inaccurate tracking data [4][8][13][14][15], complicate shape and unknown attitude evolution of the re-entering object [8][16][17][18][19], biases and stochastic inaccuracies affecting the computation of the atmospheric density at the altitudes of interest [20][21][22][23][24], magnitude, variability and prediction errors of solar and geomagnetic activity [4][8][15][16][17], and mismodeling of gas-surface interactions and drag coefficient [25][26][27].

All these uncertainty sources combine in a complex way, depending on the specific properties of the re-entering object considered and on the particular space environment conditions experienced during the final phase of the orbital decay. Therefore, even applying the same (best) models, methods and procedures, the overall relative re-entry prediction errors may be quite different for various objects and in diverse epochs. A clear example of this state of affairs is shown in Fig. 8, where the mean relative prediction errors obtained in 15 test re-entry campaigns are summarized. The re-entry prediction campaigns, involving 10 spacecraft (1, 2, 5, 6, 7, 8, 11, 13, 14, 15), 4 rocket bodies (3, 4, 9, 12) and 1 large mission related object (10), were carried out during the last 15 years (1998-2012), covering periods of high (2, 3, 4), moderate (1, 5, 13, 14, 15) and low (6, 7, 8, 9, 10, 11, 12) solar activity. All the inclinations were > 50° and 14 out of 15 objects were in nearly circular low decaying orbits. The only exception was represented by object 11, in highly elliptical Molniya orbit, whose re-entry was mainly the result of the perigee lowering induced by luni-solar gravitational perturbations, and not by atmospheric drag. The average campaign duration was about 10 days, so the total campaign averages shown in Fig. 8 refer to all the re-entry predictions computed during the last 10 days of the uncontrolled satellite lifetime. The mean relative prediction errors obtained during the last 48 hours are presented as well.

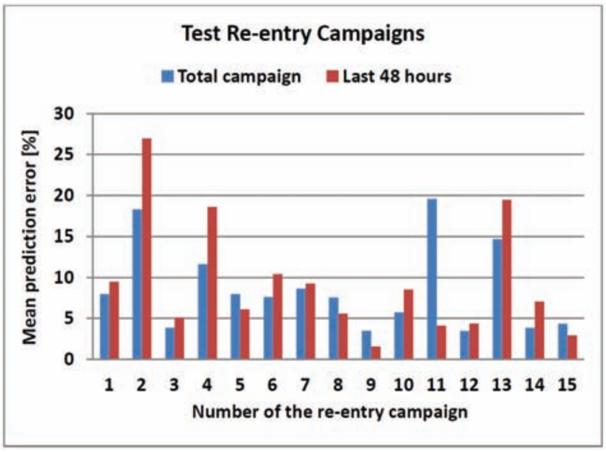

Figure 8. Mean relative prediction errors obtained in 15 test re-entry campaigns during the last 15 years (1998-2012)

In 11 out of 15 campaigns the overall mean prediction error was < 10% of the residual lifetime and in 5 cases the mean error was < 5%. In all 15 cases it was < 20%. Focusing the attention on the last 48 hours, the mean prediction error was < 5% in 4 cases, < 10% in 11 cases and < 20% in 14 out of 15 campaigns. The outlier (object 2) was a small spherical spacecraft characterized by a peculiar gas-surface interaction and this, together with quite active and variable space environment conditions, probably played a role in attaining a mean relative error of 27%.

Disregarding object 2 for the reasons just mentioned, object 11 for the highly elliptical orbit not properly managed with the methods and procedures commonly adopted for the decay from nearly circular orbits, and also object 13, for the complex shape and the huge attitude changes displayed in the last 48 hours [8], the only clear regularity emerging from Fig. 8 is that low solar and geomagnetic activity conditions, coupled with a small variability, lead to better predictions, with average relative errors of 10% or less. High solar activity and unsettled geomagnetic conditions, in particular if prone to wide variability, typically result, on the contrary, in mean relative errors of 15-20%, but with possible excursions up to 30%. This is particularly true during the last week of satellite lifetime, when an unpredicted geomagnetic storm, induced by a massive coronal mass ejection in the Sun, may produce a sensible increase of the atmospheric density at low altitude, which may persist for several hours (up to a few days), causing a sudden acceleration of the orbital decay rate and the consequent reduction of the residual lifetime. The size of the effect is a function of the geomagnetic storm severity and the satellite residual lifetime. For example, the nuclear reactor core (object C) of the satellite Cosmos 1402, at the beginning of 1983, anticipated its re-entry by nearly 14 hours in the last 3-4 days, due to the occurrence of an intense geomagnetic storm [4][16].

In conclusion, based on the results summarized in Fig. 8 and on the experience accumulated in other tens of re-entry predictions and decay analyses, a relative prediction error of at least ± 20% should be adopted to compute the uncertainty windows associated with uncontrolled satellite re-entry predictions, in order to reasonably cover all the possible error sources. However, in specific cases of high solar and geomagnetic activity, solar flare and coronal mass ejection alert and/or satellites of particularly complex shape and attitude dynamics, a more conservative prediction error of ± 25-30% should be considered, in particular during the last 2-3 days of residual lifetime [4][8][16][21][28].

5. CIVIL PROTECTION SUPPORT

In absolute terms, the amplitude of uncertainty windows depends on how far away from re-entry is the epoch of the last reliable satellite state vector used for analysis and prediction. Due to the very fast satellite velocity, this translates into huge along-track uncertainties even a few hours before an uncontrolled re-entry, as shown in Figs. 9 and 10 for a real case (Object 10 in Fig. 8). Moreover, also in the cases when the flux of orbit determinations is steady and optimal, there is an unavoidable processing and communication delay of at least 2-3 hours between the orbit determination epoch and the release of the corresponding re-entry prediction, so the final forecasts issued during the last hour or minutes preceding the actual re-entry are based on a state vector with a 2-3 hours old epoch. The consequence of this is that the predictions issued around

3 hours before re-entry have a typical along-track uncertainty of one orbit (i.e. ~40,000 km), as shown in Fig. 10, while those issued immediately before re-entry maintain a typical along-track uncertainty of half an orbit (i.e. ~20,000 km), as shown in Fig. 11 for the test case discussed. Fig. 11 also shows how the use of different standard atmospheric density models may lead to along-track differences of thousands of kilometers among the nominal impact points (COIW).

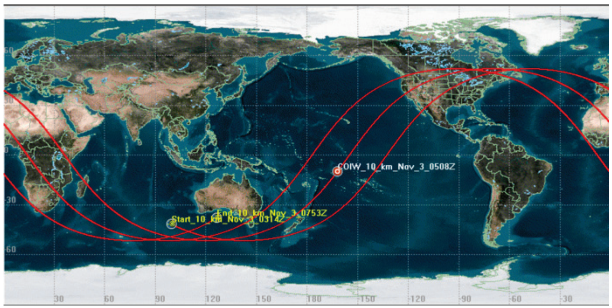

Figure 9. Sub-satellite track included in an uncertainty window computed from an orbit determined around 12 hours before re-entry by varying by ± 20% the drag perturbation

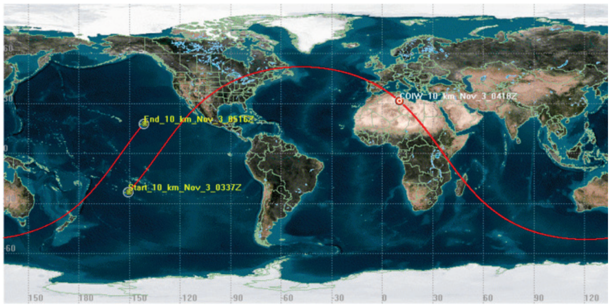

Figure 10. Sub-satellite track included in an uncertainty window computed from an orbit determined around 6 hours before re-entry by varying by ± 20% the drag perturbation

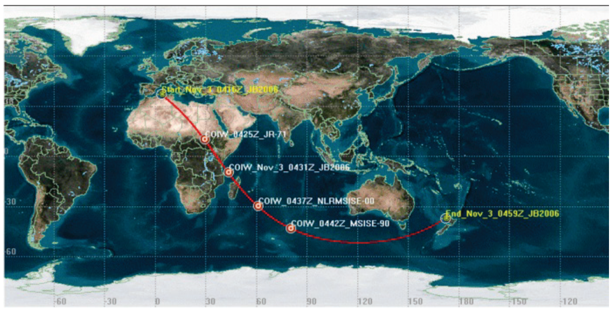

Figure 11. Final uncertainty window computed less than one hour ahead of re-entry with an orbit determined two hours before

Even though the unavoidable amplitude of the final re-entry uncertainty windows renders practically useless the nominal re-entry time for civil protection applications, the potential impact time of the fragments at a given sub-satellite location may be computed with reasonable accuracy. This allows, for any sub-satellite location included in the re-entry window, to define a risk time window. In other words, for each sub-satellite location included in the re-entry window, debris impact is possible, but not certain; however, in each place, the eventual impact may occur only during a specific risk time window, which can be therefore used to plan risk mitigation measures on the ground and in the overhead airspace. This approach has been implemented in Italy since 2003 [4][8].

Starting 3-4 days ahead of the foreseen decay, the nominal predicted trajectory is slightly modified in order to obtain simulated re-entries over Italy occurring during the current uncertainty window. The re-entry ground tracks found in this way are much more stable and less affected by propagation uncertainties, being computed with the "right" times and also including the re-entry dynamics of representative fragments up to ground impact. Nominal impact times and ground tracks are therefore integrated with a small time dispersion of a few minutes to account for initial conditions variability, a larger time dispersion of tens of minutes to account for the different flight times of fragments with distinct ballistic properties (including small particles not dangerous on the ground, but possibly representing a hazard for aircraft crossing the affected airspace), and a cross-track safety margin to account for the expected dispersion of the fragments and the trajectory residual uncertainties. The resulting risk time windows for Italy have typically an amplitude of about 30 minutes [4][8].

6. REFERENCES

1. Space Track Organization (2013). *Satellite Catalog Data*. https://www.space-track.org.

2. Klinkrad, H. (2006). *Space Debris: Models and Risk Analysis*, Springer-Verlag and Praxis Publishing Ltd, Berlin, Germany, p. 241.

3. Anselmo, L. (2012). La Militarizzazione dello Spazio. In *L'ABC del Terrore – Le Armi di Distruzione di Massa nel Terzo Millennio* (Eds. G. Giacomello & A. Pascolini), Vita & Pensiero, Milan, Italy, pp. 113–143.

4. Anselmo, L. & Pardini, C. (2005). Computational Methods for Reentry Trajectories and Risk Assessment. *Advances in Space Research* **35**(7), 1343–1352.

5. Ailor, W., Hallman, W., Steckel, G. & Weaver, M. (2005). Analysis of Reentered Debris and Implications for Survivability Modeling. In *Proc. of the Fourth European Conference on Space Debris*

(Ed. D. Danesy), ESA SP-587, ESA Publications Division, European Space Agency, Noordwijk, The Netherlands, pp. 539–544.

6. Anselmo, L., Bertotti, B. & Farinella, P. (1999). *Detriti Spaziali: Un fattore di Rischio che Incombe sul Futuro delle Attività in Orbita*, CUEN, Naples, Italy, p. 110.
7. NASA (2007). *Process for Limiting Orbital Debris*. NASA Standard 8719.14, Washington, D.C., USA.
8. Anselmo, L. & Pardini, C. (2013). Satellite Reentry Predictions for the Italian Civil Protection Authorities. *Acta Astronautica* **87**(1), 163–181.
9. Smith, P.G. (1999). *Expected Casualty Calculations for Commercial Space Launch and Reentry Missions*. Advisory Circular No. 431.35-1, Federal Aviation Administration, Washington, DC, USA.
10. Cole, J.K., Young, L.W. & Jordan-Culler, T. (1997). *Hazards of Falling Debris to People, Aircraft, and Watercraft*, Sandia Report, SAND97-0805-UC-706, Sandia National Laboratories, Albuquerque, New Mexico, USA.
11. Federal Aviation Administration (2013). *Air Traffic*. http://www.faa.gov/air_traffic/briefing/.
12. The World Bank (2013). *Air transport, registered carrier departures worldwide*. http://data.worldbank.org/indicator/IS.AIR.DPRT/countries.
13. Pardini, C. & Anselmo, L. (2004). On the Accuracy of Satellite Reentry Predictions. *Advances in Space Research* **34**(5), 1038–1043.
14. Pardini, C. & Anselmo, L. (2008). Impact of the Time Span Selected to Calibrate the Ballistic Parameter on Spacecraft Re-entry Predictions. *Advances in Space Research* **41**(7), 1100–1114.
15. Pardini, C. & Anselmo, L. (2009). USA-193 Decay Predictions with Public Domain Trajectory Data and Assessment of the Post-Intercept Orbital Debris Cloud. *Acta Astronautica* **64**(7-8), 787–795.
16. Anselmo, L. & Trumpy, S. (1986). Short-Term Predictions of Cosmos 1402 Reentry. *The Journal of the Astronautical Sciences* **34**(3), 271–285.
17. Anselmo, L., Pardini, C., Santoro, A., Trumpy, S. & Battaglia, P.E. (1991). Salyut-7/Kosmos-1686 Reentry Predictions for the Italian Civil Defence Authority. In *The Reentry of Salyut-7/Kosmos-1686* (Ed. W. Flury), ESA SP-345, ESA Publications Division, European Space Agency, Noordwijk, The Netherlands, pp. 45–50.
18. Anselmo, L., Pardini, C. & Rossi, A. (1997). Reentry Predictions for Cosmos 398, FSW-1 5 and TSS-1R. In *Proc. of the Second European Conference on Space Debris* (Ed. W. Flury), ESA SP-393, ESA Publications Division, European Space Agency, Noordwijk, The Netherlands, pp. 559–564.
19. Portelli, C., Salotti, L., Anselmo, L., Lips, T. & Tramutola, A. (2004). BeppoSAX Equatorial Uncontrolled Re-entry. *Advances in Space Research* **34**(5), 1029–1037.
20. Pardini, C. & Anselmo, L. (2001). Comparison and Accuracy Assessment of Semi-Empirical Atmosphere Models Through the Orbital Decay of Spherical Satellites. *The Journal of the Astronautical Sciences* **49**(2), 255–268.
21. Pardini, C. & Anselmo, L. (2003). Performance Evaluation of Atmospheric Density Models for Satellite Reentry Predictions with High Solar Activity Levels. *Transactions of The Japan Society for Aeronautical and Space Sciences* **46**(151), 42–46.
22. Pardini, C., Tobiska, W.K. & Anselmo, L. (2006). Analysis of the Orbital Decay of Spherical Satellites Using Different Solar Flux Proxies and Atmospheric Density Models. *Advances in Space Research* **37**(2), 392–400.
23. Pardini, C. & Anselmo, L. (2009). Performances of Atmospheric Density Models During Satellite Reentry Prediction Campaigns at Sunspot Minimum. In *Proceedings of the 21st International Symposium on Space Flight Dynamics (ISSFD-2009)*, ACM 2009-294 (CD-ROM), CNES, Toulouse, France.
24. Pardini, C., Moe, K. & Anselmo, L. (2012). Thermospheric Density Model Biases at the 23rd Sunspot Maximum. *Planetary and Space Science* **67**, 130–146.
25. Moe, K., Moe, M.M. & Wallace, S.D. (1998). Improved Satellite Drag Coefficient Calculations from Orbital Measurements of Energy Accommodation. *Journal of Spacecraft and Rockets* **35**(3), 266–272.
26. Moe, K. & Moe, M.M. (2005). Gas-surface Interactions and Satellite Drag Coefficients. *Planetary and Space Science* **53**, 793–801.
27. Pardini, C., Anselmo, L., Moe, K. & Moe, M.M. (2010). Drag and Energy Accommodation Coefficients During Sunspot Maximum. *Advances in Space Research* **45**(5), 638–650.
28. Pardini, C. & Anselmo, L. (2001). Re-entry Predictions in Support of the Inter-Agency Space Debris Coordination Committee Test Campaigns. In *Proc. of the Third European Conference on Space Debris* (Ed. H. Sawaya-Lacoste), ESA SP-473, ESA Publications Division, European Space Agency, Noordwijk, The Netherlands, Vol. 2, pp. 521–526.